Eur. Phys. J. B **37**, 169–175 (2004)
DOI: 10.1140/epjb/e2004-00043-y

THE EUROPEAN PHYSICAL JOURNAL B

Thermodynamic properties of an alternating-spin (1/2,1) two-leg ladder

X.Y. Chen[1,a], Q. Jiang[2], and W.Z. Shen[1]

[1] Laboratory of Condensed Matter Spectroscopy and Opto-Electronic Physics, Department of Physics, Shanghai Jiao Tong University, 1954 Hua Shan Road, Shanghai 200030, P.R. China
[2] Department of Physics, Suzhou University, Suzhou, 215006, P.R. China

Received 2 April 2003 / Received in final form 24 October 2003
Published online 15 March 2004 –

Abstract. With the aid of the Schwinger-boson mean-field method, we study the low-lying excitations and thermodynamic properties of a ferrimagnetic Heisenberg two-leg ladder (i.e., a ferrimagnetic double-chain with an antiferromagnetic interaction). The interaction between the two chains plays an important role in producing a low-lying excitation energy gap, affecting the low-lying excited spectrum, and increasing the disorder of the ferrimagnetic double-chain. The excitation spectrum, energy gap, and spin reduction in the ground state are calculated. Thermodynamic quantities such as the short-range spin correlation and short-range order are also obtained at low temperatures. In this gapful system, we observed the exponential behaviors in both the specific heat (C_V) and the product of magnetic susceptibility and temperature (χT) at low temperatures. The exponential behavior of the χT versus temperature agrees qualitatively with the experimental results in $NiCu(pba)(D_2O)_3 \cdot D_2O$ at low temperatures.

PACS. 75.10.Jm Quantized spin models – 75.40.Cx Static properties (order parameter, static susceptibility, heat capacities, critical exponents, etc.) – 75.50.Ee Antiferromagnetics – 75.50.Gg Ferrimagnetics

1 Introduction

The field of low-dimensional quantum-spin systems has been a focus in condensed-matter physics for about two decades since Haldane pointed out the difference between the integer-spin Heisenberg-antiferromagnetic chains and the half-integer spin chains. By mapping the Heisenberg antiferromagnetic chain to a nonlinear sigma model, Haldane conjectured that there is a finite gap between the ground state and the low-lying excitation states for the chains with integer spin, while there is no gap for half-integer spin chains [1]. This conjecture had been verified by later analytic, numerical, and experimental studies. Current interests have spread into wider classes of spin ladders, stimulated by the experimental realization of a variety of spin systems [2]. These spin ladders consist of coupled one-dimensional chains, which can be classified as a uniform-spin ladder and alternating-spin ladder. Theoretical studies [3–5] have suggested that there are two different universal classes for the uniform-spin ladders, i.e., the antiferromagnetic spin-1/2 ladders are gapful or gapless depending on whether n (the number of legs) is even or odd. These predictions have been confirmed experimentally on $LaCuO_{2.5}$ [6], and $SrCu_2O_3$ [7].

It is very interesting to predict a similar phenomenon in the alternating-spin Heisenberg ladders by spin wave mean-field theory (SWMFT) [8], in which the interaction between two ferrimagnetic Heisenberg chains would also send the double-chain into a new disordered phase. This gapful phase was proved further by the nonlinear sigma model [8] and the density matrix renormalization group (DMRG) [9]. However, up to now, corresponding analytic work is still relatively limited, especially in comparison with the uncoupled ferrimagnetic chains. Experimentally, the family of compounds of $ACu(pba)(H_2O)_3 \cdot H_2O$ (with A = Mn, Fe, Co, Ni, and pba = 1,3-propylenebisoxamato) belongs to the weakly coupled alternating spin chains family [10], in which the interchain coupling plays an important role at extremely low temperature. These have motivated us to study the low-temperature thermodynamic properties in such a mixed-spin two-leg ladder system composed of two ferrimagnetic Heisenberg chains with two kinds of spins $S^A = 1/2$ and $S^B = 1$. This "ferrimagnetic Heisenberg two-leg ladder" has isotropic couplings J_1 along the chains and J_2 between them. The Hamiltonian of this model is represented by:

$$H = J_1 \sum \left(S_{2i}^{A_1} \cdot S_{2i+1}^{B_1} + S_{2i}^{A_2} \cdot S_{2i+1}^{B_2} \right) + J_2 \sum \left(S_{2i}^{A_1} \cdot S_{2i}^{A_2} + S_{2i+1}^{B_1} \cdot S_{2i+1}^{B_2} \right), \quad (1)$$

[a] e-mail: rom@wx88.net

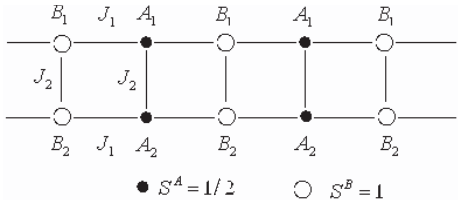

Fig. 1. The ferrimagnetic Heisenberg two-leg ladder model. The open (filled) circles represent S^A=1/2 (S^B=1) spins. A_1, A_2, B_1, and B_2 specify four spins in the unit cell. The system contains N such unit cells.

with the corresponding configuration shown in Figure 1. In this paper, we limit our discussions to the effect of the interchain coupling J_2 in this paper, accepting that $J_1 = 1$.

As we know, the SWMFT, in dealing with the low-lying excitation spectrum, was successfully used in a one-dimensional spin (1,1/2) ferrimagnetic Heisenberg chain and gave results in good agreement with those from the DMRG [11,12]. However, for this two-leg ladder system, the SWMFT is successful only in obtaining the linear excitation spectrum through predicting a new disordered phase caused by the intrachain coupling as we have mentioned above, but fails to predict the spin gap [8]. It is the interchain coupling that destroys the long-range order in the ground state of the ferrimagnetic single-chain, and drives the system into a spin liquid phase. Consequently, the SWMFT's assumption of the long-range order in the ground state breaks down, and the SWMFT is not suitable for the ferrimagnetic Heisenberg two-leg ladder. Unlike the SWMFT, the Schwinger-boson approach (SBMFT) is a powerful technique [13], which provides a useful starting point to characterize the spin liquid and valence bond states as the nonvanishing expectation value of the mean field contributed from a *bondvariable*, representing the short-range correlations without assuming any long-range order. Obviously, the SBMFT is very effective due to the existence of the short-range antiferromagnetic correlations in the mixed spin system. It has been successfully applied in a one-dimensional ferrimagnetic Heisenberg chain [14] and a two-dimensional mixed-spin model on square lattice [15]. Therefore, we may employ it in this middle case (between one-dimension and two-dimension) of the "ferrimagnetic Heisenberg two-leg ladder".

In this paper, the SBMFT is employed to describe the two-leg ladder ranging from the weak coupling regime ($J_2 = 0$) to the strong coupling regime ($J_2 = 1$). The excitation spectrum, energy gap, and spin reduction in the ground state are investigated in detail, which are in good agreement with those from the DMRG by Trumper and Gazza in reference [9]. Furthermore, the thermodynamic quantities of the energy gaps, short-range spin correlations, and short-range orders are discussed at low temperatures. The low-temperature magnetic susceptibility and specific heat are also calculated and compared with the experimental results.

This paper is organized as follows. In Section 2, we introduce briefly the Schwinger-boson techniques that we use in this paper. In Section 3, we discuss the thermodynamic properties in the ground state and at low temperatures. A brief summary is given at the end.

2 Schwinger-boson mean field theory

The four spin operators $S_1^{A_n}$ and $S_1^{B_n}$ in equation (1) can be represented by eight kinds of Schwinger bosons ($a_{l,\uparrow}^{(1)} a_{l,\downarrow}^{(1)} a_{l,\uparrow}^{(2)} a_{l,\downarrow}^{(2)}$), and ($b_{l,\uparrow}^{(1)} b_{l,\downarrow}^{(1)} b_{l,\uparrow}^{(2)} b_{l,\downarrow}^{(2)}$) on their sublattices,

$$S_{l,+}^{A_n} = a_{l,\uparrow}^{(n)+} a_{l,\downarrow}^{(n)} \; S_{l,z}^{A_n} = \tfrac{1}{2}\left(a_{l,\uparrow}^{(n)+} a_{l,\uparrow}^{(n)} - a_{l,\downarrow}^{(n)+} a_{l,\downarrow}^{(n)} \right) \quad (2)$$

$$S_{l,+}^{B_n} = b_{l,\uparrow}^{(n)+} b_{l,\downarrow}^{(n)} \; S_{l,z}^{B_n} = \tfrac{1}{2}\left(b_{l,\uparrow}^{(n)+} b_{l,\uparrow}^{(n)} - b_{l,\downarrow}^{(n)+} b_{l,\downarrow}^{(n)} \right), \quad (3)$$

where $n = 1$ and 2 represent the up chain and the down chain, respectively. On each sublattice, it should be constrained by the conditions: $a_{l,\uparrow}^{(n)+} a_{l,\uparrow}^{(n)} + a_{l,\downarrow}^{(n)+} a_{l,\downarrow}^{(n)} = 2S^A$ (for $l = 2i$) and $b_{l,\uparrow}^{(n)+} b_{l,\uparrow}^{(n)} + b_{l,\downarrow}^{(n)+} b_{l,\downarrow}^{(n)} = 2S^B$ (for $l = 2i+1$). By imposing the constraints on each site, we can correctly map the original spin system to a bosonic system. Introducing four Lagrange multipliers λ_{A_n} and λ_{B_n} for the sublattices of A_n and B_n, respectively, we can obtain the mean field Hamiltonian within the above constraints:

$$\begin{aligned} H^{MF} = {} & \lambda_{A_1} \sum_i \left[a_{2i,\uparrow}^{(1)+} a_{2i,\uparrow}^{(1)} + a_{2i,\downarrow}^{(1)+} a_{2i,\downarrow}^{(1)} - 2S^{A_1} \right] \\ & + \lambda_{A_2} \sum_i \left[a_{2i,\uparrow}^{(2)+} a_{2i,\uparrow}^{(2)} + a_{2i,\downarrow}^{(2)+} a_{2i,\downarrow}^{(2)} - 2S^{A_2} \right] \\ & + \lambda_{B_1} \sum_i \left[b_{2i,\uparrow}^{(1)+} b_{2i,\uparrow}^{(1)} + b_{2i,\downarrow}^{(1)+} b_{2i,\downarrow}^{(1)} - 2S^{B_1} \right] \\ & + \lambda_{B_2} \sum_i \left[b_{2i,\uparrow}^{(2)+} b_{2i,\uparrow}^{(2)} + b_{2i,\downarrow}^{(2)+} b_{2i,\downarrow}^{(2)} - 2S^{B_2} \right] \\ & + J_1 \sum_{i,\eta} \left[S^{A_1} S^{B_1} - 2A_{2i,2i+\eta}^{+} A_{2i,2i+\eta} + S^{A_2} S^{B_2} \right. \\ & \left. -2B_{2i,2i+\eta}^{+} B_{2i,2i+\eta} \right] + J_2 \sum_i \left[S^{A_1} S^{A_2} - C_{2i}^{+} C_{2i} \right. \\ & \left. + S^{B_1} S^{B_2} - D_{2i+1}^{+} D_{2i+1} \right], \end{aligned} \quad (4)$$

where the four bond operators used in the above equation are introduced as:

$$\begin{aligned} A_{2i,2i+\eta} &= \tfrac{1}{2}\left(a_{2i,\uparrow}^{(1)} b_{2i+\eta,\downarrow}^{(1)} - a_{2i,\downarrow}^{(1)} b_{2i+\eta,\uparrow}^{(1)} \right) \\ B_{2i,2i+\eta} &= \tfrac{1}{2}\left(a_{2i,\uparrow}^{(2)} b_{2i+\eta,\downarrow}^{(2)} - a_{2i,\downarrow}^{(2)} b_{2i+\eta,\uparrow}^{(2)} \right) \\ C_{2i} &= \tfrac{1}{2}\left(a_{2i,\uparrow}^{(1)} a_{2i,\downarrow}^{(2)} - a_{2i,\downarrow}^{(1)} a_{2i,\uparrow}^{(2)} \right) \\ D_{2i+1} &= \tfrac{1}{2}\left(b_{2i+1,\uparrow}^{(1)} b_{2i+1,\downarrow}^{(2)} - b_{2i+1,\downarrow}^{(1)} b_{2i+1,\uparrow}^{(2)} \right). \end{aligned} \quad (5)$$

Considering the symmetry between the up chain and the down chain in the ladder, we take the thermal average $\langle A_{2i,2i+1} \rangle = \langle B_{2i,2i+1} \rangle = A e^{i\theta_A}$, $\langle C_{2i} \rangle = C e^{i\theta_C}$ and $\langle D_{2i+1} \rangle = D e^{i\theta_D}$. Here A, C, and D are three real amplitudes of short-range order (SRO) parameters, reflecting

the strength of the short-range antiferromagnetic correlations in the sublattices of $(A_n - B_n)$, $(A_1 - A_2)$, and $(B_1 - B_2)$, respectively, with their corresponding phase factors θ_A, θ_C, and θ_D. It was the three non-zero SRO parameters that enabled us to use the SBMFT. These will be explained in the following section. Since $\lambda_{A_1} = \lambda_{A_2}$ and $\lambda_{B_1} = \lambda_{B_2}$ for the same reason of symmetry, we can rewrite them as λ_A and λ_B, respectively. Thus under the Hartree-Fock approximation, we can reduce the above effective Hamiltonian to:

$$
\begin{aligned}
H^{MF} &= 4NJ_1S^AS^B + NJ_2S^AS^A + NJ_2S^BS^B + 8NJ_1A^2 \\
&+ 2NJ_2C^2 + 2NJ_2D^2 - 4N\lambda_AS^A - 4N\lambda_BS^B \\
&+ \lambda_A \sum_k \left[a_{k,\uparrow}^{(1)+}a_{k,\uparrow}^{(1)} + a_{k,\downarrow}^{(1)+}a_{k,\downarrow}^{(1)} + a_{k,\uparrow}^{(2)+}a_{k,\uparrow}^{(2)} + a_{k,\downarrow}^{(2)+}a_{k,\downarrow}^{(2)}\right] \\
&+ \lambda_B \sum_k \left[b_{k,\uparrow}^{(1)+}b_{k,\uparrow}^{(1)} + b_{k,\downarrow}^{(1)+}b_{k,\downarrow}^{(1)} + b_{k,\uparrow}^{(2)+}b_{k,\uparrow}^{(2)} + b_{k,\downarrow}^{(2)+}b_{k,\downarrow}^{(2)}\right] \\
&- J_1 \sum_k \left[z\gamma_k A e^{-i\theta_A}\left(a_{k,\uparrow}^{(1)}b_{k,\downarrow}^{(1)} - a_{k,\downarrow}^{(1)}b_{k,\uparrow}^{(1)}\right)\right. \\
&\left. + z\gamma_k A e^{i\theta_A}\left(a_{k,\uparrow}^{(1)+}b_{k,\downarrow}^{(1)+} - a_{k,\downarrow}^{(1)+}b_{k,\uparrow}^{(1)+}\right)\right] \\
&- J_1 \sum_k \left[z\gamma_k A e^{-i\theta_A}\left(a_{k,\uparrow}^{(2)}b_{k,\downarrow}^{(2)} - a_{k,\downarrow}^{(2)}b_{k,\uparrow}^{(2)}\right)\right. \\
&\left. + z\gamma_k A e^{i\theta_A}\left(a_{k,\uparrow}^{(2)+}b_{k,\downarrow}^{(2)+} - a_{k,\downarrow}^{(2)+}b_{k,\uparrow}^{(2)+}\right)\right] \\
&- J_2 \sum_k \left[C e^{-i\theta_C}\left(a_{k,\uparrow}^{(1)}a_{k,\downarrow}^{(2)} - a_{k,\downarrow}^{(1)}a_{k,\uparrow}^{(2)}\right)\right. \\
&\left. + C e^{i\theta_C}\left(a_{k,\uparrow}^{(1)+}a_{k,\downarrow}^{(2)+} - a_{k,\downarrow}^{(1)+}a_{k,\uparrow}^{(2)+}\right)\right] \\
&- J_2 \sum_k \left[D e^{-i\theta_D}\left(b_{k,\uparrow}^{(1)}b_{k,\downarrow}^{(2)} - b_{k,\downarrow}^{(1)}b_{k,\uparrow}^{(2)}\right)\right. \\
&\left. + D e^{i\theta_D}\left(b_{k,\uparrow}^{(1)+}b_{k,\downarrow}^{(2)+} - b_{k,\downarrow}^{(1)+}b_{k,\uparrow}^{(2)+}\right)\right] \qquad (6)
\end{aligned}
$$

where $\sum_k$ is the sum of k over the first Brillouin zone. The structure factor γ_k is defined as: $\gamma_k = \frac{1}{z}\sum_{\eta=\pm1} e^{i\eta k}$ with z the number of nearest neighbors, and η the nearest neighbor site.

By diagonalizing the mean-field Hamiltonian via the Bogliubov transformation we can have:

$$
\begin{aligned}
H^{MF} &= E_{const} \\
&+ \sum_k \left[E^-(k)\left(\alpha_{k,\uparrow}^{(1)+}\alpha_{k,\uparrow}^{(1)} + \beta_{k,\downarrow}^{(1)+}\beta_{k,\downarrow}^{(1)} + 1\right.\right. \\
&\left.\left. + \beta_{k,\uparrow}^{(2)+}\beta_{k,\uparrow}^{(2)} + \alpha_{k,\downarrow}^{(2)+}\alpha_{k,\downarrow}^{(2)} + 1\right)\right] + \sum_k \left[E^+(k)\left(\alpha_{k,\downarrow}^{(1)+}\alpha_{k,\downarrow}^{(1)}\right.\right. \\
&\left.\left. + \beta_{k,\uparrow}^{(1)+}\beta_{k,\uparrow}^{(1)} + 1 + \beta_{k,\downarrow}^{(2)+}\beta_{k,\downarrow}^{(2)} + \alpha_{k,\uparrow}^{(2)+}\alpha_{k,\uparrow}^{(2)} + 1\right)\right] \\
&= E_{const} + 2\sum_k \left[E^-(k)\left(2n_k^- + 1\right)\right. \\
&\left. + E^+(k)\left(2n_k^+ + 1\right)\right], \qquad (7)
\end{aligned}
$$

with

$$
\begin{aligned}
E_{const} &= 4NJ_1S^AS^B + NJ_2\left(S^AS^A + S^BS^B\right) \\
&+ 8NJ_1A^2 + 2NJ_2\left(C^2 + D^2\right) \\
&- 2N\lambda_A\left(2S^A + 1\right) - 2N\lambda_B\left(2S^B + 1\right).
\end{aligned}
$$

For each k, there are eight branches of spectra, four of each have the same size of excitation energy. They can be divided into two classes: one belongs to the acoustic branch $E^-(k)$, the other to the optical branch $E^+(k)$. From a statistical point of view, we have $\langle\alpha_{k,\uparrow}^{(1)+}\alpha_{k,\uparrow}^{(1)}\rangle = \langle\beta_{k,\downarrow}^{(1)+}\beta_{k,\downarrow}^{(1)}\rangle = \langle\beta_{k,\uparrow}^{(2)+}\beta_{k,\uparrow}^{(2)}\rangle = \langle\alpha_{k,\downarrow}^{(2)+}\alpha_{k,\downarrow}^{(2)}\rangle$ and $\langle\alpha_{k,\downarrow}^{(1)+}\alpha_{k,\downarrow}^{(1)}\rangle = \langle\beta_{k,\uparrow}^{(1)+}\beta_{k,\uparrow}^{(1)}\rangle = \langle\beta_{k,\downarrow}^{(2)+}\beta_{k,\downarrow}^{(2)}\rangle = \langle\alpha_{k,\uparrow}^{(2)+}\alpha_{k,\uparrow}^{(2)}\rangle$. Therefore, we can rewrite them as n_k^- and n_k^+, respectively, which are the Bose-type quasi-particles with energies of $E^-(k)$ and $E^+(k)$. The corresponding excitation spectra are:

$$
E^-(k) = \sqrt{\tfrac{E_0 - \sqrt{E_1}}{2}},\ E^+(k) = \sqrt{\tfrac{E_0 + \sqrt{E_1}}{2}}, \qquad (8)
$$

$$
\begin{aligned}
E_0 &= \lambda_A^2 + \lambda_B^2 - 2\left(2J_1A\cos[k]\right)^2 - (J_2C)^2 - (J_2D)^2 \\
E_1 &= \left(\lambda_A^2 - \lambda_B^2 - (J_2C)^2 + (J_2D)^2\right) \\
&- 4(2J_1A\cos[k])^2\left((\lambda_A - \lambda_B)^2 - (J_2C)^2 - (J_2D)^2\right. \\
&\left. - 2J_2^2CD\cos[2\theta_A - \theta_C - \theta_D]\right). \qquad (9)
\end{aligned}
$$

In the meantime, we define the two energy gaps as follows:

$$
\Delta^- = 2Min[E^-(k)],\ \Delta^+ = 2Min[E^+(k)], \qquad (10)
$$

where Δ^- and Δ^+ are the energy gaps of the acoustic spectrum $E^-(k)$ and the optical spectrum $E^+(k)$, respectively.

By minimizing the free energy obtained from equations (7–9) at finite temperatures, we end up with a group of self-consistent equations for the eight parameters of A, C, D, λ_A, λ_B, θ_A, θ_C and θ_D. To our delight, the three self-consistent equations about θ_A, θ_C and θ_D can be simplified by $\theta_A = \theta_C = \theta_D = 0$, or π, which means that $\langle A_{2i,2i+1}\rangle$, $\langle C_{2i}\rangle$ and $\langle D_{2i+1}\rangle$ are real numbers. The final simplified self-consistent equations are:

$$
\begin{aligned}
1 + 2S^A &= \frac{2}{\pi}\int_0^{\frac{\pi}{2}}\left[\coth\left(\frac{E^-(k)}{2T}\right)\frac{\partial E^-(k)}{\partial\lambda_A}\right. \\
&\left. + \coth\left(\frac{E^+(k)}{2T}\right)\frac{\partial E^+(k)}{\partial\lambda_A}\right]dk \qquad (11)
\end{aligned}
$$

$$
\begin{aligned}
1 + 2S^B &= \frac{2}{\pi}\int_0^{\frac{\pi}{2}}\left[\coth\left(\frac{E^-(k)}{2T}\right)\frac{\partial E^-(k)}{\partial\lambda_B}\right. \\
&\left. + \coth\left(\frac{E^+(k)}{2T}\right)\frac{\partial E^+(k)}{\partial\lambda_B}\right]dk \qquad (12)
\end{aligned}
$$

$$
\begin{aligned}
-8J_1A &= \frac{2}{\pi}\int_0^{\frac{\pi}{2}}\left[\coth\left(\frac{E^-(k)}{2T}\right)\frac{\partial E^-(k)}{\partial A}\right. \\
&\left. + \coth\left(\frac{E^+(k)}{2T}\right)\frac{\partial E^+(k)}{\partial A}\right]dk \qquad (13)
\end{aligned}
$$

$$-2J_2C = \frac{2}{\pi}\int_0^{\frac{\pi}{2}} \left[\coth\left(\frac{E^-(k)}{2T}\right)\frac{\partial E^-(k)}{\partial C} + \coth\left(\frac{E^+(k)}{2T}\right)\frac{\partial E^+(k)}{\partial C}\right] dk \quad (14)$$

$$-2J_2D = \frac{2}{\pi}\int_0^{\frac{\pi}{2}} \left[\coth\left(\frac{E^-(k)}{2T}\right)\frac{\partial E^-(k)}{\partial D} + \coth\left(\frac{E^+(k)}{2T}\right)\frac{\partial E^+(k)}{\partial D}\right] dk, \quad (15)$$

where T is the reduced temperature (i.e., $k_B = 1$), and $E^{\pm}(k)$ are formulated in equations (8–9). Given the interacting couplings J_1 and J_2, we can solve the above self-consistent equations (11–15) to acquire the short-range order parameters of A, C, and D, and determine the two energy spectra $E^-(k)$ and $E^+(k)$ at finite temperature T. In the ground state, the term of $\coth(\frac{E^{\xi}(k)}{2T})$ can be reduced to 1 as long as a finite gap exists in the spectrum of $E^{\xi}(k)$ (here $\xi = +$ or $-$). The Bogliubov transformation can also be obtained after solving these self-consistent equations, which relates the original quasi-particle operators ($a^{(n)}_{k,\sigma}$ and $b^{(n)}_{k,\sigma}$, $\sigma = \uparrow$ or $\downarrow$) in equation (6) with the new quasi-particle operators ($\alpha^{(n)}_{k,\sigma}$ and $\beta^{(n)}_{k,\sigma}$) in equation (7), and can be used to calculate the average value of the z-direction sublattice spin and the corresponding nearest neighbor correlations. The four spin reductions on the four sublattice sites in the unit cell are defined as:

$$\tau_{A_n} = S^A - (-1)^n\langle S_z^{A_n}\rangle, \tau_{B_n} = S^B - (-1)^n\langle S_z^{B_n}\rangle \quad (\text{for } n = 1,\ 2). \quad (16)$$

3 Numerical results and discussion

3.1 Properties in the ground state

We start first our discussion with the extreme case of a ferrimagnetic single chain at $J_2 = 0$, which has been proved to has a gapless acoustic spectrum and a gapful optical spectrum [11,14]. In the case of $J_2 = 0$, we can reduce the above equations (8–9) by $C = D = 0$, which compare with reference [14]. It should be taken into account that the Bogliubov quasi-particle condensation in the n_k^- channel of equation (7) would take place at absolute zero temperature, because the excitation energy $E^-(k)$ has its minimal value $E^-(k) = 0$ at $k = 0$. But no condensation happens in the n_k^+ channel because of a finite optical gap. These have been described in detail in references [14] and [15]. In the ground state of the ferrimagnetic single chain, two z-direction sub-lattice spins are obtained as: $\langle S^A_{2i,z}\rangle = -0.291$ and $\langle S^B_{2i+1,z}\rangle = 0.791$, and the ferrimagnetic long-range order persists [14]. The spin reduction on the A site $\tau_A = S^A + \langle S^A_z\rangle$ is equal to that on the B site $\tau_B = S^B - \langle S^B_z\rangle = 0.209$. It is very interesting to discuss the effects of the interchain interaction J_2 on these special characteristics in a ferrimagnetic double-chain.

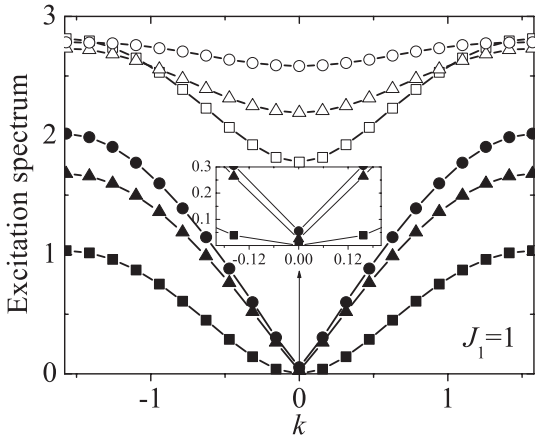

Fig. 2. The excitation spectra of $E^-(k)$ (filled points) and $E^+(k)$ (open points) as a function of k at J_1=1. The square curve, triangle curve, and circle curve correspond to the cases of J_2=0, 0.6, and 1, respectively. Shown in the inset is the enlargement around the center of the first Brillouin zone, displaying the linear k relation with a finite energy gap.

When $J_2 = 0$, our results agree with reference [14] as we remarked above, and the lower energy spectrum in the low-k regime would have a square formula as $E^-(k \to 0) \sim v_s k^2$. However, any antiferromagnetic interaction between the two ferrimagnetic chains would drive the system into the gapful phase, which has an approximate acoustic spectrum of the form $E^-(|k| < 1) \sim \sqrt{(\frac{\Delta^-}{2})^2 + v^2k^2}$ from the above equations (8–10). But this spectrum approaches the nearly linear relation $v|k|$ for the k in the center of Brillouin zone owing to the small gap, as shown in Figure 2. Figure 2 shows the excitation spectra at three different cases of J_2 for fixed $J_1 = 1$. At $J_2 = 0$, the system is returned to the isolated ferrimagnetic chains, the gapless acoustic dispersion simply follows the k^2 dependence, which is denoted by the filled square curve. However, the acoustic spectra displays an approximately linear k relation in the center of the first Brillouin zone for $|k| < 1$ with a very small gap at $J_2 = 0.6$ and $J_2 = 1$, which are marked by the filled triangle curve and filled circle curve, respectively. The linear acoustic spectrum is an important feature of the disordered ground state in many antiferromagnetic systems, which was pointed out by Fukui and Kawakami in reference [8]. In addition, the increase of the coupling constant J_2 enhances the bandwidth of the acoustic spectrum, but contracts the bandwidth of the optical spectrum. This phenomenon has also been observed in two-dimensional ($S^A = 1$, $S^B = 1/2$) mixed-spin systems [15], which is a signal that the one-dimensional two-leg ladder is a crossover between the one- and two-dimensional cases.

It was the interchain interaction that drives the system into a gapful phase. This interaction should have a significant effect on the both gaps of the acoustic and optical spectrum. Figure 3 shows the two gaps of Δ^- (acoustic spectrum gap) and Δ^+ (optical spectrum gap) as a function of J_2 in the regime of $0 < J_2 < 1$, respectively. Both

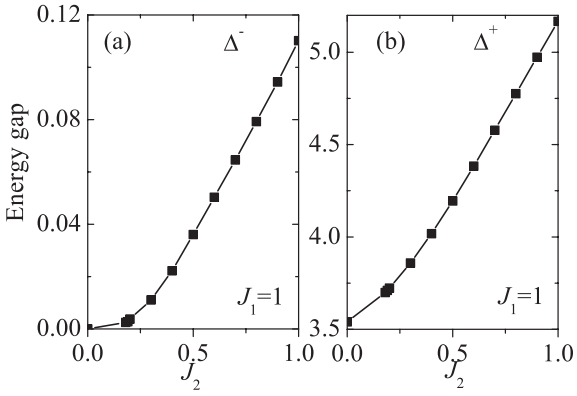

Fig. 3. The energy gaps of (a) Δ^- and (b) Δ^+ as a function of the interchain interaction J_2 for $J_1 = 1$.

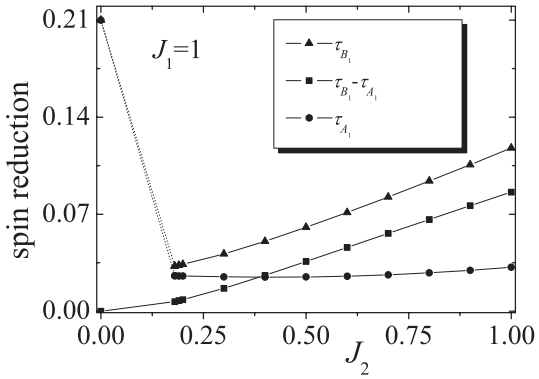

Fig. 4. Spin reductions in the ground state as a function of the interchain interaction J_2.

the acoustic gap and optical gap show a linear relation with the interaction between the two ferrimagnetic chains when the interaction J_2 is larger than 0.4, but a quadratic relation in the weak interaction case. These conclusions are in agreement with the results of the DMRG [9], which further ensures us that the SBMFT is effective for this mixed spin system.

Due to the interchain interaction, the ground state of the double-chain becomes the singlet state in the gapful phase. From the above Bogliubov transformation between equations (6) and (7), we can obtain $\langle S^{A_1}_{2i,z}\rangle = -\langle S^{A_2}_{2i,z}\rangle$ and $\langle S^{B_1}_{2i+1,z}\rangle = -\langle S^{B_2}_{2i+1,z}\rangle$, which result in an antiferromagnetic ground state with the z-directional total spin in the unit cell $S_{tot} = \langle S^{A_1}_{2i,z} + S^{B_1}_{2i+1,z} + S^{A_2}_{2i,z} + S^{B_2}_{2i+1,z}\rangle = 0$ as presented by Trumper and Gazza in reference [9]. According to the above definitions in equation (16), the four spin reductions on the double-chain are also symmetric (i.e., $\tau_{A_1} = \tau_{A_2}$ and $\tau_{B_1} = \tau_{B_2}$). Figure 4 shows the two spin reductions about τ_{A_1} and τ_{B_1} as function of the interaction J_2, which are denoted by the filled circle and triangular curve, respectively. The two equal spin reductions at $J_2 = 0$ decrease quickly with increasing J_2 in the range of $0 \leq J_2 < 0.18$, which is the transition of the double-chain from the ferrimagnetic phase to the gapful phase. The above self-consistent equations (11–15) have no real number solutions for $0 < J_2 < 0.18$, so our mean-field

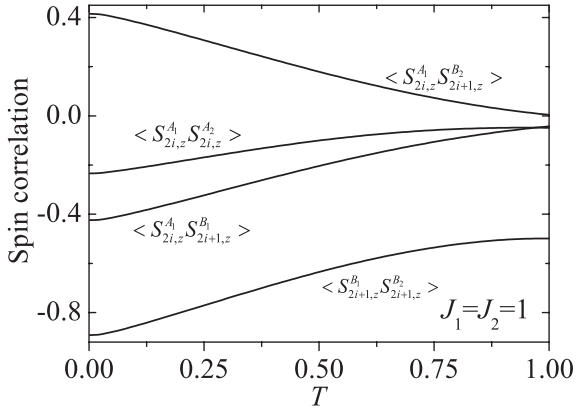

Fig. 5. Temperature-dependent SRO parameters (A, C, and D) for the interaction couplings $J_1 = J_2 = 1$.

approach is not good enough to describe this phase transition in weak-coupling regimes, as shown by the dotted curve in Figure 4. When the interaction J_2 is above 0.18, the two spin reductions become separated, and increase to different degrees with the increase of J_2. The spin reduction of τ_{B_1} increases more quickly than τ_{A_1} due to the larger spin magnitude on the B sublattice. In the mean time, the long-range staggered ferrimagnetic order in one leg of the two-leg ladder system is not completely destroyed. $\tau_{B_1} - \tau_{A_1} = 1/2 - \langle S^{A_1}_{2i,z} + S^{B_1}_{2i+1,z}\rangle$ reflects the disorder of the system, which is shown by the square curve in Figure 4. With the increase of the interchain interaction J_2, the ground state of the ferrimagnetic double-chain becomes more disordered. The enlargement of the gap and disorder in the ground state with the increase of the interaction J_2 means an increase of the antiferromagnetic correlation, which will be discussed below.

3.2 Properties at low temperatures

Now, we move to the thermodynamic properties at finite temperatures for the special case of $J_1 = J_2 = 1$. Four kinds of sublattice spin correlations in the z-direction (i.e., $\langle S^{A_1}_{2i,z} S^{A_2}_{2i,z}\rangle$, $\langle S^{B_1}_{2i+1,z} S^{B_2}_{2i+1,z}\rangle$, $\langle S^{A_1}_{2i,z} S^{B_1}_{2i+1,z}\rangle$ and $\langle S^{A_1}_{2i,z} S^{B_2}_{2i+1,z}\rangle$) are calculated at low temperatures, which are shown in Figure 5. In the antiferromagnetic ground state ($T = 0K$), the first three kinds are negative, which shows that the two nearest-neighbor sublattice spins are staggered with respect to each other in the z-direction, and the positive $\langle S^{A_1}_{2i,z} S^{B_2}_{2i+1,z}\rangle$ shows the spins on the sublattices of $(A_1 - B_2)$ are parallel in the z-direction. These conclusions are in agreement with the above antiferromagnetic configuration in the ground state. Meanwhile, Figure 5 clearly illustrates that all four kinds of short-range correlations are decreased by thermal fluctuations, demonstrating that the short-range order will decrease with an increase in the temperature.

From equation (5), we know the strengths of the above three short-range correlations (i.e., $\langle S^{A_1}_{2i,z} S^{A_2}_{2i,z}\rangle$, $\langle S^{B_1}_{2i+1,z} S^{B_2}_{2i+1,z}\rangle$, and $\langle S^{A_1}_{2i,z} S^{B_1}_{2i+1,z}\rangle$) can be represented

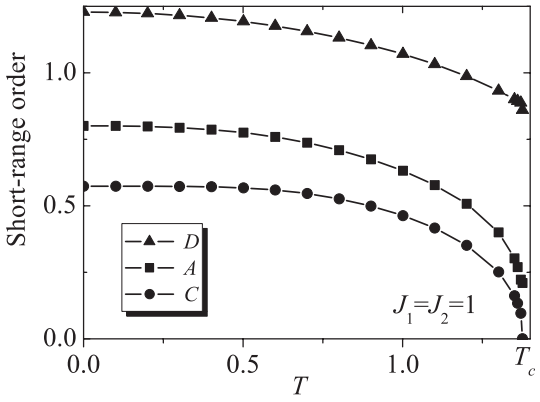

Fig. 6. Four short-range spin correlations of $\langle S^{A_1}_{2i,z} S^{A_2}_{2i,z}\rangle$, $\langle S^{B_1}_{2i+1,z} S^{B_2}_{2i+1,z}\rangle$, $\langle S^{A_1}_{2i,z} S^{B_1}_{2i+1,z}\rangle$ and $\langle S^{A_1}_{2i,z} S^{B_2}_{2i+1,z}\rangle$ versus temperature T.

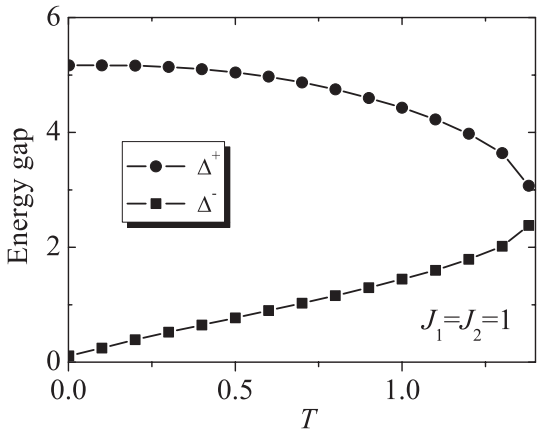

Fig. 7. Temperature-dependent energy gaps of Δ^- and Δ^+ for the special case where $J_1 = J_2 = 1$.

by three SRO parameters (C, A, and D), respectively. Figure 6 shows the calculated results for the three SRO parameters (C, A, and D) at low temperatures. With an increase in the temperature, all three SRO parameters decrease, reflecting that the strengths of the short-range antiferromagnetic correlations in the sublattices of $(A_1 - A_2)$, $(A_n - B_n)$ and $(B_1 - B_2)$ become weaker. Over the whole temperature range in Figure 6, we can see $D > A > C$, which shows that both the magnitude of short-range correlation and the SRO parameter depend on the magnitude of the corresponding sublattice spins, as pointed out in reference [9]. Consequently, the SRO parameter C is the smallest one among them, and becomes zero first when the temperature approaches the cross-temperature T_c. Here the cross-temperature T_c in this two-leg ladder system cannot be expressed by a simple formula, and we only have the numerical value of $T_c \simeq 1.376$. The existence of the above SRO parameters and corresponding short-range correlations below T_c are the foundation of the SBMFT. Once the temperature is above T_c, the above SRO breaks down, resulting in the failure of the SBMFT, as already pointed out in references [14,15].

The temperature-dependent energy gaps have been plotted in Figure 7. With the increase in the temperature, the two gaps vary in different ways: the acoustic gap becomes bigger, while the optical gap becomes smaller. This is a universal phenomenon in the mixed-spin system regardless of the dimension of the system. This phenomenon has also been observed in both the one-dimensional mixed-spin system [14] and the two-dimensional mixed-spin system [15].

The specific heat C_V can be obtained by the numerical differentiation of the internal energy with respect to T. From the Bogliubov transformation, we can also obtain the per unit cell magnetic susceptibility χ under zero magnetic field at a finite temperature:

$$\chi = \frac{1}{k_B T} \sum_{n=1,2}^{\xi=\uparrow,\downarrow} \left[\left\langle \alpha^{(n)+}_{k,\xi} \alpha^{(n)}_{k,\xi} \right\rangle \left(\left\langle \alpha^{(n)+}_{k,\xi} \alpha^{(n)}_{k,\xi} \right\rangle + 1 \right) + \left\langle \beta^{(n)+}_{k,\xi} \beta^{(n)}_{k,\xi} \right\rangle \left(\left\langle \beta^{(n)+}_{k,\xi} \beta^{(n)}_{k,\xi} \right\rangle + 1 \right) \right].$$

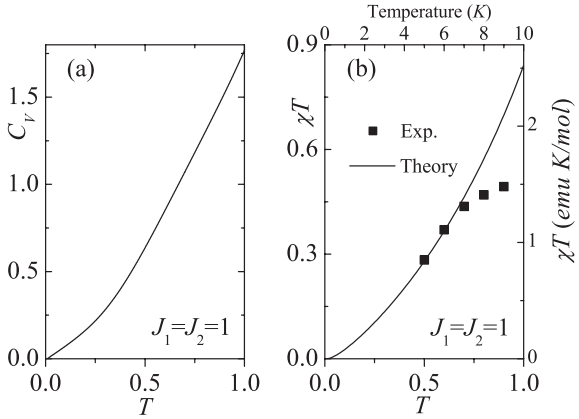

Fig. 8. The per unit cell specific heat C_V (a) and the product of the magnetic susceptibility and temperature χT (b) versus T. The experimental results of $NiCu(pba)(D_2O)_3 \cdot D_2O$ in reference [17] have been plotted as filled squares in (b) with the temperature in K and χT in emu K/mol.

Here we use the reduced temperature (i.e., $k_B = 1$). In such a gapful system, both the specific heat C_V and the product of magnetic susceptibility and temperature χT show an exponential relation with temperature T, as shown in Figures 8a and b, respectively. These are the basic features in the gapful phase. It should be noted that the steep decrease of χT had been observed in the experiments on $NiCu(pba)(D_2O)_3 \cdot D_2O$ below $T = 7$ K [17], which is caused by interchain antiferromagnetic couplings. For a direct comparison with the experiment results, we have also plotted the experimental results in Figure 8b as filled squares. Our theoretical results, solid line in Figure 8b, can explain qualitatively the exponential temperature behavior of χT as the temperature goes down to zero. The small divergence with the temperature above $T = 7$ K is due to the weakness or even disappearance of the interchain interaction, while the temperature-dependent interchain interaction has not been taken into account in our theoretical calculations.

4 Conclusions

In summary, the thermodynamic properties in the system of a quantum ferrimagnetic double-chain have been investigated in detail, and are affected by two main factors of interchain coupling J_2 and temperature T. In one special case where $J_2 = 0$, we compare our results with the earlier conclusions in reference [14], which provide a good physical picture. In another special case where $J_2 = 1$, the reasonable result for the gap $\Delta^- = 0.11$ is good enough to recall the generalization suggested by Haldane concerning the antiferromagnetic coupling system in ferrimagnetic systems, though it is smaller than that of 0.33 from the DMRG. The interchain interaction of J_2 can send the quantum mixed-spin system into a gapful phase. Our results support the suggestion by Trumper and Gazza in reference [9] that for a ferrimagnetic multi-chain, any odd number of chains always has a ferrimagnetic gapless ground state which is ordered, any even number of chains has a spin gap behavior analogous to the uniform spin-1/2 case.

Furthermore, this paper provides a good evidence for the theoretical spin gap caused by the interchain interaction in the ferrimagnetic ladder. Thermodynamic observables of C_V and χT are calculated, which take on the typical characteristics found in the Haldane gap systems, i.e., the exponential temperature-dependent behavior. Especially, the theoretically temperature-dependent χT explains well the experimental results on $NiCu(pba)(D_2O)_3 \cdot D_2O$ below $T = 7$ K [17]. The ground-state energy gap and the band gap are also discussed, which may have some special effects on its magnetization plateau curve at $T = 0$ K. However, these are beyond the scope of this paper and will be considered in the future.

This work was supported in part by the Natural Science Foundation of China under the contract of 10125416.

References

1. F.D.M. Haldane, Phys. Rev. Lett. **50**, 1153 (1983); F.D.M. Haldane, Phys. Lett. A **93**, 464 (1983)
2. R.J. Cava et al., J. Solid State Chem. **94**, 170 (1991)
3. A.A. Zvyagin, Sov. J. Low Temp. Phys. **18**, 558 (1992)
4. D.V. Khveshchenko, Phys. Rev. B **50**, 380 (1994)
5. G. Sierra, J. Phys. A **29**, 3299 (1996)
6. S. Sugai, T. Shinoda, N. Kobayashi, Z. Hiroi, M. Takano, Phys. Rev. B **60**, R6969 (1999)
7. E. Dagotto, Rep. Prog. Phys. **62**, 1525 (1999)
8. T. Fukui, N. Kawakami, Phys. Rev. B **57**, 398 (1998)
9. A.E. Trumper, C. Gazza, Phys. Rev. B **64**, 134408 (2001)
10. Van Koningsbruggen, O. Kahn, K. Nakatani, Y. Pei, J.P. Renard, Inorg. Chem. **29**, 3325 (1990); O. Kahn, Y. Pei, M. Verdaguer, J.P. Renard, J. Sletten, J. Am. Chem. Soc. **110**, 782 (1988)
11. S.K. Pati, S. Ramasesha, D. Sen, Phys. Rev. B **55**, 8894 (1997)
12. S. Brehmer, H.J. Mikeska, S. Yamamoto, J. Phys. Condens. Matter **9**, 3921 (1997)
13. D.P. Arovas, A. Auerbach, Phys. Rev. B **38**, 316 (1988)
14. C.J. Wu, B. Chen, X. Dai, Y. Yu, Z.B. Su, Phys. Rev. B **60**, 1057 (1999)
15. Y. Takushima, A. Koga, N. Kawakami, Phys. Rev. B **61**, 15189 (2000)
16. A.K. Kolezhuk, H.J. Mikeska, S. Yamamoto, Phys. Rev. B **55**, R3336 (1997)
17. M. Hagiwara, K. Minami, Y. Narumi, K. Tatani, K. Kindo, J. Phys. Soc. Jpn **67**, 2209 (1998)